J|A|C|S
ARTICLES
Published on Web 01/24/2006

Thermodynamics of Interactions of Water-Soluble Porphyrins with RNA Duplexes

Ara A. Ghazaryan,[†] Yeva B. Dalyan,[†] Samvel G. Haroutiunian,[†] Anna Tikhomirova,[‡] Nicolas Taulier,[‡] James W. Wells,[‡] and Tigran V. Chalikian*,[‡]

Contribution from the Department of Molecular Physics, Faculty of Physics, Yerevan State University, 1 Alex Manoogian Street, Yerevan 375025, Armenia, and Department of Pharmaceutical Sciences, Leslie Dan Faculty of Pharmacy, University of Toronto, 19 Russell Street, Toronto, Ontario M5S 2S2, Canada

Received July 5, 2005; E-mail: chalikan@phm.utoronto.ca

Abstract: We characterized the interactions of *meso*-tetrakis(4*N*-(2-hydroxyethyl)pyridinium-4-yl) porphyrin (TEtOHPyP4), *meso*-tetrakis(4*N*-allylpyridinium-4-yl) porphyrin (TAlPyP4), and *meso*-tetrakis(4*N*-metallylpyridinium-4-yl) porphyrin (TMetAlPyP4) with the poly(rA)poly(rU) and poly(rI)poly(rC) RNA duplexes between 18 and 45 °C by employing circular dichroism, light absorption, and fluorescence intensity spectroscopic measurements. Our results suggest that TEtOHPyP4 and TAlPyP4 intercalate into the poly(rA)poly(rU) and poly(rI)poly(rC) host duplexes, while TMetAlPyP4 associates with these RNA duplexes by forming outside-bound, self-stacked aggregates. We used our temperature-dependent absorption titration data to determine the binding constants and stoichiometry for each porphyrin−RNA binding event studied in this work. From the temperature dependences of the binding constants, we calculated the binding free energies, ΔG_b, enthalpies, ΔH_b, and entropies, ΔS_b. For each RNA duplex, the binding enthalpy, ΔH_b, is the most favorable for TEtOHPyP4 (an intercalator) followed by TAlPyP4 (an intercalator) and TMetAlPyP4 (an outside binder). On the other hand, for each duplex, external self-stacking of TMetAlPyP4 produces the most favorable change in entropy, ΔS_b, followed by the intercalators TAlPyP4 and TEtOHPyP4. Thus, our results suggest that the thermodynamic profile of porphyrin−RNA binding may correlate with the binding mode. This correlation reflects the differential nature of molecular forces that stabilize/destabilize the two modes of binding—intercalation versus external self-stacking along the host duplex.

Introduction

Cationic porphyrins have emerged as a promising yet relatively untapped class of DNA-binding molecules with potential applications in biology and medicine, in particular, as potent anti-viral and anti-tumor therapeutic agents.[1,2] As DNA-binding ligands, porphyrins are quite unusual; they may associate with DNA in three distinct binding modes, which include intercalation, groove binding, and outside binding with self-stacking along the DNA helix.[1,3−5] The binding mode of a specific porphyrin−nucleic acid system depends on chemical features of the porphyrin and the structure and composition of the host DNA and RNA.

The majority of porphyrin−DNA studies have focused on *meso*-tetrakis(*N*-methylpyridinium-4-yl) porphyrin (H_2TMPyP) and its metal derivatives.[1,3−9] This porphyrin contains four positively charged pyridinium residues with methyl peripheral substituents. These studies have provided us with valuable information about the sequence-specific and ligand-specific binding preferences of H_2TMPyP4 and its metaloderivatives as well as the binding constants and the binding stoichiometry of porphyrin−DNA interactions. In particular, it has been shown that H_2TMPyP4 selectively intercalates in GC-rich regions of duplex DNA, while binding externally in regions with a high percentage of AT base pairs.[4] Association of H_2TMPyP4 with RNA duplexes has been studied by Uno et al.[8] H_2TMPyP4 binds externally to the poly(rG)poly(rC) and poly(rI)poly(rC) duplexes.[8] Upon associating with poly(rA)poly(rU), H_2TMPyP4 exhibits two modes of binding. At low drug-to-RNA ratios, H_2TMPyP4 binds externally to poly(rA)poly(rU), while at high drug-to-RNA ratios, it intercalates.[8] Interestingly, substitution of methyl peripheral substituents with bulkier 2-hydroxyethyl and propyl groups does not alter the binding pattern and preferences of the porphyrins with respect to GC-rich and AT-rich DNA domains.[10,11] There are no data about the influence

[†] Yerevan State University.
[‡] University of Toronto.

(1) Marzilli, L. G. *New J. Chem.* **1990**, *14*, 409−420.
(2) Villanueva, A.; Juarranz, A.; Diaz, V.; Gomez, J.; Canete, M. P. *Anti-Cancer Drug Des.* **1992**, *7*, 297−303.
(3) Fiel, R. J. *J. Biomol. Struct. Dyn.* **1989**, *6*, 1259−1275.
(4) Pasternack, R. F.; Gibbs, E. J.; Villafranca, J. J. *Biochemistry* **1983**, *22*, 2406−2414.
(5) Pasternack, R. F.; Gibbs, E. J. *Met. Ions Biol. Syst.* **1996**, *33*, 367−397.
(6) Haq, I.; Trent, J. O.; Chowdhry, B. Z.; Jenkins, T. C. *J. Am. Chem. Soc.* **1999**, *121*, 1768−1779.
(7) Pasternack, R. F.; Gibbs, E. J.; Villafranca, J. J. *Biochemistry* **1983**, *22*, 5409−5417.
(8) Uno, T.; Hamasaki, K.; Tanigawa, M.; Shimabayashi, S. *Inorg. Chem.* **1997**, *36*, 1676−1683.
(9) Uno, T.; Aoki, K.; Shikimi, T.; Hiranuma, Y.; Tomisugi, Y.; Ishikawa, Y. *Biochemistry* **2002**, *41*, 13059−13066.
(10) Kuroda, R.; Takahashi, E.; Austin, C. A.; Fisher, L. M. *FEBS Lett.* **1990**, *262*, 293−298.

10.1021/ja054070n CCC: $33.50

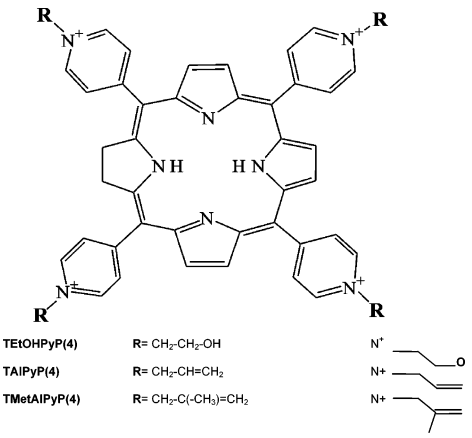

Figure 1. Chemical structure of the porphyrins.

of bulky peripheral substituents on the binding of porphyrins to RNA duplexes. This deficiency is unfortunate since chemical modification of peripheral groups is one logical way of improving the affinity and specificity of DNA- and RNA-binding porphyrins.

In this work, we investigate the RNA-binding properties of water-soluble porphyrins with bulky peripheral substituents. Specifically, we study interactions of *meso*-tetrakis(4*N*-(2-hydroxyethyl)pyridinium-4-yl) porphyrin (TEtOHPyP4), *meso*-tetrakis(4*N*-allylpyridinium-4-yl) porphyrin (TAlPyP4), and *meso*-tetrakis(4*N*-metallylpyridinium-4-yl) porphyrin (TMetAlPyP4) (see Figure 1) with the poly(rA)poly(rU) and poly(rI)poly(rC) homopolymeric RNA duplexes. To this end, we perform temperature-dependent light absorption, circular dichroism (CD), and fluorescence titration experiments. We use our spectroscopic data to determine the binding constants, K_b, for each porphyrin−RNA binding event under study as a function of temperature. Further, we use the van't Hoff equation to calculate the binding enthalpies, ΔH_b, from the temperature dependences of K_b. We calculate the binding entropies, ΔS_b, from the binding free energies, $\Delta G_b = -RT\ln K_b$, and enthalpies, ΔH_b, using $\Delta S_b = (\Delta H_b - \Delta G_b)/T$. Our spectroscopic data reveal that TEtOHPyP4 and TAlPyP4 intercalate between bases of the poly(rA)poly(rU) and poly(rI)poly(rC) duplexes. In contrast, TMetAlPyP4 associates with the two RNA duplexes by forming external stacks along their helices. Significantly, we find that our measured thermodynamic profiles may correlate with the mode of porphyrin−RNA association. This correlation may reflect the differential nature of the molecular forces that are involved in stabilizing/destabilizing the two binding modes—intercalation versus outside stacking.

Materials and Methods

Materials. *Meso*-tetrakis(4*N*-(2-hydroxyethyl)pyridinium-4-yl) porphyrin (TEtOHPyP4), *meso*-tetrakis(4*N*-allylpyridinium-4-yl) porphyrin (TAlPyP4), and *meso*-tetrakis(4*N*-metallylpyridinium-4-yl) porphyrin (TMetAlPyP4) were synthesized, purified, and kindly donated by Dr. Robert Ghazaryan (Faculty of Pharmaceutical Chemistry, Yerevan State University, Armenia). Poly(rI)poly(rC) was obtained from Sigma-Aldrich Canada (Oakville, ON, Canada). The single-stranded poly(rA) and poly(rU) RNA polymers were purchased from Amersham Pharmacia Biotech, Inc. (Baie d'Urfé, Québec, Canada). These polymers were of the highest grade commercially available and used without further purification. Equimolar amounts of the poly(rA) and poly(rU) single strands were mixed in buffer to obtain the poly(rA)poly(rU) duplex. The concentrations of the single- and double-stranded polynucleotides were determined spectrophotometrically using the following molar extinction coefficients (expressed per nucleotide): poly(rA), $\epsilon_{258} = 9800\ M^{-1}\ cm^{-1}$; poly(rU), $\epsilon_{260} = 9350\ M^{-1}\ cm^{-1}$; poly(rA)poly(rU), $\epsilon_{257} = 7000\ M^{-1}\ cm^{-1}$; and poly(rI)poly(rC), $\epsilon_{266} = 5250\ M^{-1}\ cm^{-1}$. The concentrations of the porphyrins were determined using the following molar extinction coefficients: TEtOHPyP4, $\epsilon_{422} = 2.26 \times 10^5\ M^{-1}\ cm^{-1}$; TAlPyP4, $\epsilon_{424} = 2.23 \times 10^5\ M^{-1}\ cm^{-1}$; and TMetAlPyP4, $\epsilon_{424} = 2.16 \times 10^5\ M^{-1}\ cm^{-1}$.

All measurements were performed in a pH 7.0 buffer consisting of 10 mM sodium phosphate, 185 mM NaCl, and 1 mM Na_2EDTA. RNA samples were dissolved in the buffer and exhaustively dialyzed at 4 °C against the same buffer using a dialysis tubing with a molecular weight cut off of 1000 Da (Spectrum, Houston, TX) for at least 24 h. The ligand solutions were prepared before each experiment by dissolving the porphyrin in the dialysate. Porphyrin solutions were kept in the dark all the time.

Circular Dichroism Spectroscopy. CD spectra of the RNA duplexes in the absence and presence of the porphyrins were recorded at 25 °C using an AVIV model 62 DS spectropolarimeter (Aviv Associates, Lakewood, NJ). An optical cuvette with a 1 cm path length was used for all CD measurements. CD titration profiles were measured by adding aliquots of a porphyrin to a known amount of RNA solution. The initial RNA concentrations were in the range of 50 to 100 μM.

Visible Absorption Spectrophotometry. Visible absorption spectra of the porphyrins were measured in the Soret region in the absence and presence of the RNA duplexes. Data were collected at 18, 25, 35, and 45 °C using an AVIV model 14 DS UV/vis spectrophotometer (Aviv Associates, Lakewood, NJ) and an optical cuvette with a path length of 1 cm. All absorption titrations were carried out by the stepwise addition of aliquots of a stock solution of RNA to a cuvette containing 1 mL of a solution of porphyrin at an initial concentration of ~5 μM. At each point in the titration, the total concentration of porphyrin was corrected for the increase in volume upon the addition of RNA. All three porphyrins were tested for conformity with the Beer−Lambert law. In each case, the absorption between 300 and 500 nm was found to increase linearly with the concentration of porphyrin over the range used in the experiments.

The binding of porphyrin to RNA was monitored by the absorption at either 422 nm (TEtOHPyP4 and TAlPyP4) or 425 nm (TMetAlPyP4), which corresponds to λ_{max} for the Soret band of the free porphyrin. The data were assessed in terms of the noncooperative neighbor-exclusion model,[12] as represented by eq 1.[13]

$$C_f = -r\left[\frac{(n-1)r-1}{nr-1}\right]^n [K_b((n-1)r-1)]^{-1} \qquad (1)$$

The parameter K_b in eq 1 represents the equilibrium association constant for the binding of porphyrin to RNA; n is the number of base pairs that are occluded by the interaction and thereby rendered inaccessible to subsequent equivalents of the ligand. The variable C_f represents the free concentration of porphyrin, which is given by $C_f = (1 - \alpha)C_t$. In the latter expression, C_t represents the total concentration of porphyrin, and α is the fraction of total porphyrin bound to RNA. The value of α was calculated from the equation $\alpha = (A_{free} - A)/(A_{free} - A_{sat})$, where A is the absorption at any concentration of RNA over the course of titration; A_{free} represents the absorption in the absence of RNA, and A_{sat} is the asymptotic value of A at concentrations of RNA sufficient to bind all of the porphyrin (i.e., $[RNA] \gg K_b^{-1}$). The quantity r in eq 1 represents the binding ratio and is given by $r = (C_t - C_f)/[RNA]$, where [RNA] is the total concentration of RNA in the cuvette. Equation 1 can be rearranged to obtain eq 2, in which both the porphyrin and

(11) Gray, T. A.; Yue, K. T.; Marzilli, L. G. *J. Inorg. Biochem.* **1991**, *41*, 205−219.
(12) McGhee, J. D.; von Hippel, P. H. *J. Mol. Biol.* **1974**, *86*, 469−489.
(13) Correia, J. J.; Chaires, J. B. *Methods Enzymol.* **1994**, *240*, 593−614.

RNA enter as total concentration:

$$f(A) = -A + A_{sat} - \frac{(A_{free} - A)}{K_b[RNA]} \times \frac{[(n-1)r-1]^{n-1}}{(nr-1)^n} \quad (2)$$

where

$$r = \frac{\alpha C_t}{[RNA]} \equiv \frac{A_{free} - A}{A_{free} - A_{sat}} \times \frac{C_t}{[RNA]}$$

Estimates of the absorption at graded concentrations of RNA were analyzed in terms of eq 2 to obtain fitted values of K_b, n, A_{free}, and A_{sat}. The value of A at each step of the titration was obtained as the appropriate root, which was computed numerically by means of the Newton−Raphson procedure combined with bracketing and bisection.[14] Successive estimates of A require the first derivative of eq 2; that is

$$\frac{df(A)}{dA} = -1 - \frac{1}{K_b[RNA]} \times \frac{[(n-1)r-1]^{n-1}}{(nr-1)^n} \times \left(1 - \frac{nr}{nr-1} + \frac{(n-1)r}{(n-1)r-1}\right) \quad (3)$$

The upper bracket on the value of A was taken as A_{free}, and the lower bracket was taken as the greater of A_{sat} or A_{min} as defined in eq 4 [i.e., $nr = 1$ or $(n-1)r = 1$]. Owing to the high levels of mutual depletion between the porphyrin and RNA under some conditions, it proved necessary to carry out the calculation in double precision.

$$A_{min} = A_{free} - \frac{[RNA]}{C_t} \times \frac{A_{free} - A_{sat}}{n} \quad (4)$$

The parameters K_b, n, A_{free}, and A_{sat} were optimized by nonlinear regression, and values at successive iterations of the fitting procedure were adjusted according to the algorithm of Marquardt.[15] The dissociation constant was optimized as either K_b or log K_b, as required. With any particular ligand interacting with either poly(rA)poly(rU) or poly(rI)poly(rC) the data obtained at all four temperatures were analyzed in concert. Within such analyses, the curve at each temperature made a comparable contribution to the global sum of squares. Estimates of parametric error were calculated from the diagonal elements of the covariance matrix at the minimum in the sum of squares. Other details regarding the statistical procedures have been described elsewhere.[16]

Preliminary analyses indicated that the values of K_b, n, and A_{sat} tend to be highly correlated when the data acquired at each temperature with a particular ligand and RNA are treated independently, that is, when a separate value of each parameter is assigned to each set of data. It therefore was assumed that temperature was without effect on the number of base pairs occluded by the ligand, and a single value of n was shared among the four sets of data obtained with the same ligand and either poly(rA)poly(rU) or poly(rI)poly(rC). The data obtained at each temperature were assigned separate values of K_b, A_{free}, and A_{sat}. This constraint on n reduced or eliminated the correlations between n and K_b, and the latter could be assessed independently of the former.

Fluorescence Spectroscopy. Emission spectra were recorded at 18, 25, 35, and 45 °C using an AVIV model ATF 105 spectrofluorometer (Aviv Associates, Lakewood, NJ) with a bandwidth adjusted to 2 nm. The fluorescence titration experiments were performed in a 1 cm path length cuvette by adding aliquots of RNA to a known amount of the ligand (~7 μM). The excitation wavelengths were adjusted to 400 (TEtOHPyP4 and TAlPyP4) and 438 (TMetAlPyP4) nm, while the emission spectra were collected from 620 to 850 nm.

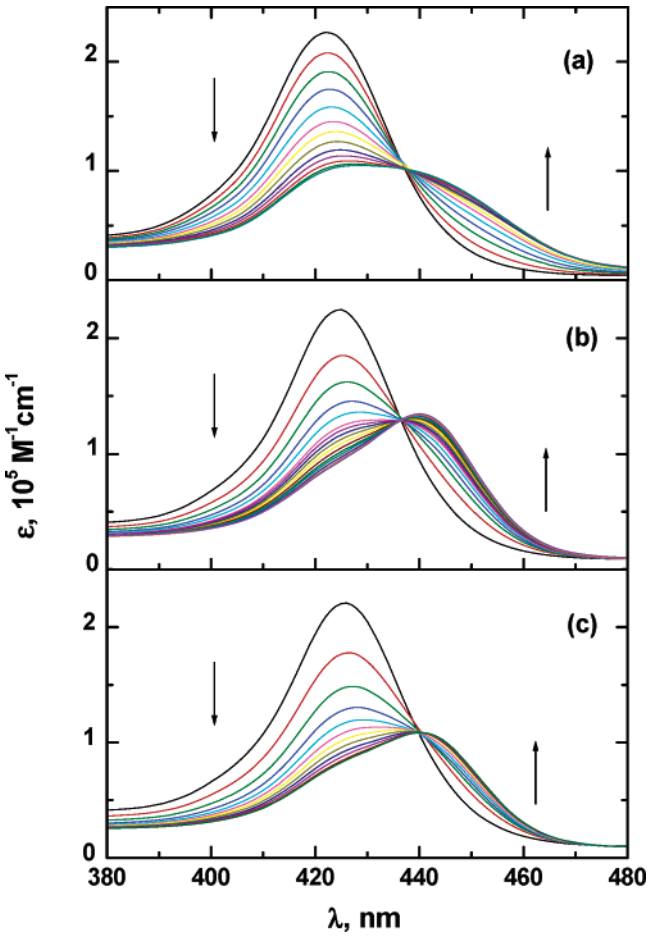

Figure 2. Visible absorption spectra of TEtOHPyP4 (panel a), TAlPyP4 (panel b), and TMetAlPyP4 (panel c) in the absence and presence of poly(rA)poly(rU) at 25 °C. The initial concentrations of the porphyrins were ~5 μM. The final RNA-to-ligand ratios were 10.4, 26.1, and 38.1 for TEtOHPyP4, TAlPyP4, and TMetAlPyP4, respectively. The individual values of the final RNA-to-ligand ratio for each titration were selected to ensure saturation of the binding profiles.

Results

We recorded light absorption spectra in the Soret region for the three porphyrins in the presence and absence of the poly(rA)poly(rU) and poly(rI)poly(rC) duplexes at 18, 25, 35, and 45 °C. Figure 2 shows how the visible spectra of TEtOHPyP4 (panel A), TAlPyP4 (panel B), and TMetAlPyP4 (panel C) in the Soret region change upon addition of poly(rA)poly(rU) at a representative temperature of 25 °C. Figure 3 shows the spectral changes of TEtOHPyP4 (panel A), TAlPyP4 (panel B), and TMetAlPyP4 (panel C) in the presence of poly(rI)poly(rC) at 25 °C. Inspection of Figures 2 and 3 reveals that each ligand−RNA binding event studied here is characterized by a substantial hypochromicity and red shift of the Soret maximum. Another important feature of the plots shown in Figures 2 and 3 is the presence of isosbestic points (between 435 and 440 nm), an observation consistent with a single binding mode.

Fluorescence emission spectra of the three porphyrins in the Q-band region in the presence and absence of the poly(rA)poly(rU) and poly(rI)poly(rC) duplexes were collected at 18, 25, 35, and 45 °C. Figures 4 and 5 show these spectra for

(14) Press, W. H.; Teukolsky, S. A.; Vetterling, W. T.; Flannery, B. P. *Numerical Recipes in FORTRAN: The Art of Scientific Computing*, 2nd ed.; Cambridge University Press: Cambridge, 1992.
(15) Marquardt, D. W. *J. Soc. Ind. Appl. Math.* **1963**, *11*, 431−441.
(16) Wells, J. W. In *Receptor−Ligand Interactions: A Practical Approach*; Hulme, E. C., Ed.; Oxford University Press: Oxford, 1992; pp 289−395.

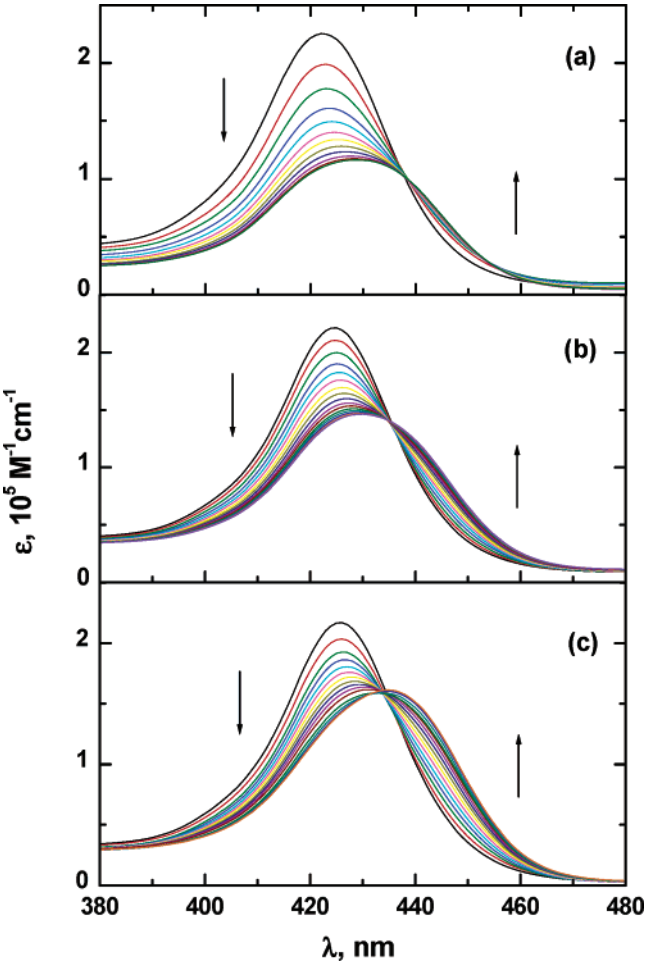

Figure 3. Visible absorption spectra of TEtOHPyP4 (panel a), TAlPyP4 (panel b), and TMetAlPyP4 (panel c) in the absence and presence of poly(rI)poly(rC) at 25 °C. The initial concentrations of the porphyrins were ~5 μM. The final RNA-to-ligand ratios were 20.6, 60.9, and 65.2 for TEtOHPyP4, TAlPyP4, and TMetAlPyP4, respectively. The individual values of the final RNA-to-ligand ratio for each titration were selected to ensure saturation of the binding profiles.

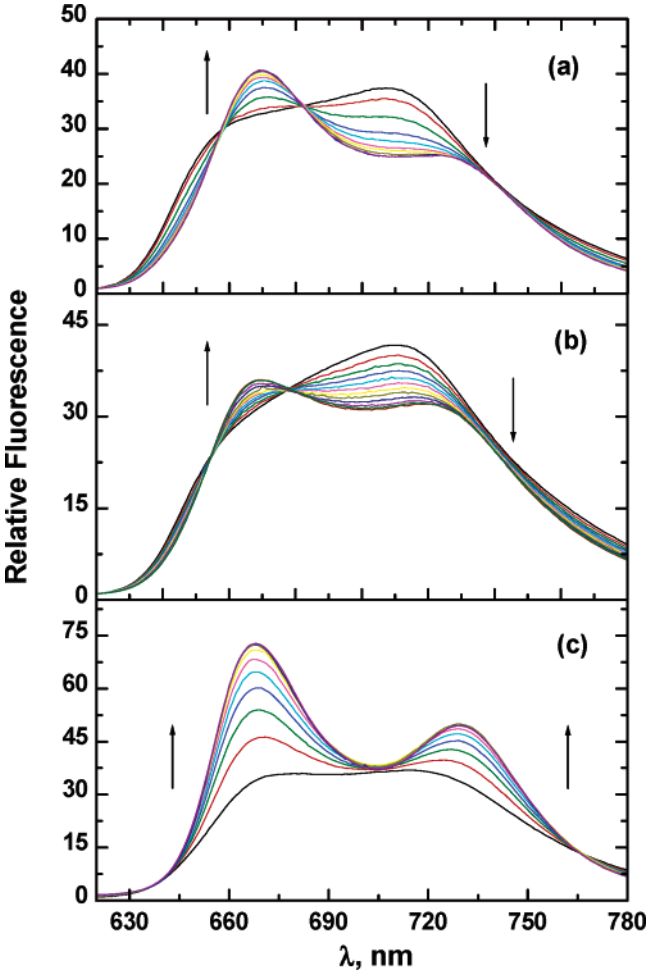

Figure 4. Fluorescence intensity spectra of TEtOHPyP4 (panel a), TAlPyP4 (panel b), and TMetAlPyP4 (panel c) in the absence and presence of poly(rA)poly(rU) at 25 °C. The initial concentrations of the porphyrins were ~7 μM. The final RNA-to-ligand ratios were 9.3, 21.8, and 37.9 for TEtOHPyP4, TAlPyP4, and TMetAlPyP4, respectively. The individual values of the final RNA-to-ligand ratio for each titration were selected to ensure saturation of the binding profiles.

TEtOHPyP4 (panels A), TAlPyP4 (panels B), and TMetAlPyP4 (panels C) interacting with poly(rA)poly(rU) (Figure 4) or poly(rI)poly(rC) (Figure 5) at a representative temperature of 25 °C. Analogous to the absorption spectra, the fluorescence spectra all exhibit one or more isoemissive points. This observation lends further support to the notion that all porphyrin−RNA association events studied in this work involve a single binding mode.

Figure 6 presents the CD spectra of poly(rA)poly(rU) (panel A) and poly(rI)poly(rC) (panel B) saturated with TEtOHPyP4, TAlPyP4, and TMetAlPyP4. Inspection of Figure 6a reveals that the CD spectrum of poly(rA)poly(rU) associated with TMetAlPyP4 is qualitatively and quantitatively distinct from the spectra exhibited by the complexes with TEtOHPyP4 and TAlPyP4. Specifically, the TMetAlPyP4−poly(rA)poly(rU) complex exhibits a much larger signal in the RNA region and a strong conservative band in the Soret region. Similar observations can be made for the porphyrin−poly(rI)poly(rC) complexes in Figure 6b.

We used Soret absorption data at 422 (TEtOHPyP4 and TAlPyP4) and 425 (TMetAlPyP4) nm to construct the binding profiles for each porphyrin−RNA binding event studied in the present paper. These profiles were analyzed numerically with the neighbor-exclusion model (see Materials and Methods). Figure 7 shows representative binding profiles for TEtOHPyP4 association with poly(rA)poly(rU) and poly(rI)poly(rC) obtained at 25 °C. Figure 8 plots the logarithms of the binding constants, $\ln K_b$, against reciprocal temperature, $1/T$, for the association of the porphyrins with poly(rA)poly(rU) (panel A) and poly(rI)poly(rC) (panel B), respectively. These experimental dependences were approximated by linear functions; the slopes of these functions yield the binding enthalpies, $\Delta H_b = -R[\partial \ln K_b/\partial(1/T)]_P$. The binding free energies, ΔG_b, and entropies, ΔS_b, were calculated using $\Delta G_b = -RT\ln K_b$ and $\Delta S_b = (\Delta H_b - \Delta G_b)/T$. Tables 1 and 2 present our evaluated thermodynamic parameters for the association of the porphyrins with poly(rA)poly(rU) and poly(rI)poly(rC), respectively.

Discussion

Modes of Binding. The three modes of binding of porphyrins to nucleic acids are reflected in and can be discriminated based on characteristic changes in visible absorbance and induced CD spectra in the Soret region as well as fluorescence intensity spectra in the Q-band region.[1,3,4,7,17,18] Intercalation is character-

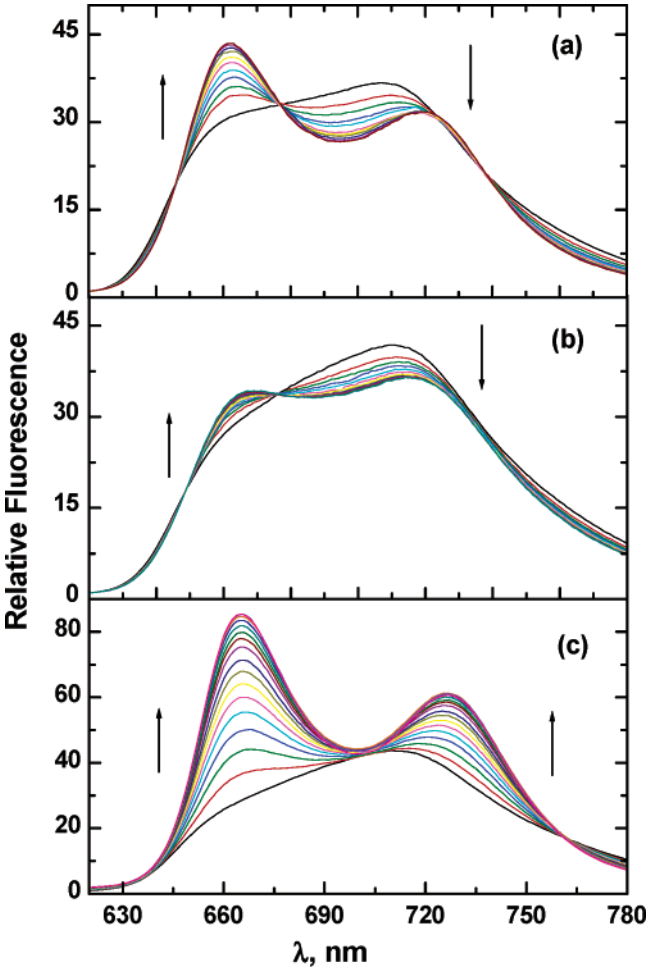

Figure 5. Fluorescence intensity spectra of TEtOHPyP4 (panel a), TAlPyP4 (panel b), and TMetAlPyP4 (panel c) in the absence and presence of poly(rI)poly(rC) at 25 °C. The initial concentrations of the porphyrins were ~7 μM. The final RNA-to-ligand ratios were 18.5, 59.6, and 50.4 for TEtOHPyP4, TAlPyP4, and TMetAlPyP4, respectively. The individual values of the final RNA-to-ligand ratio for each titration were selected to ensure saturation of the binding profiles.

ized by a large bathochromic effect and hypochromicity of the Soret band and negative induced CD band in the Soret region. Groove binding exhibits a moderate bathochromic shift and hypochromicity of the Soret band and a positive induced CD band in the Soret region. The most distinctive diagnostic property of outside binding with porphyrin stacking is a strong conservative CD band in the Soret region, while changes in the Soret band are less conclusive.

Inspection of graphs a−c in Figure 2 reveals that the binding of the porphyrins to poly(rA)poly(rU) is accompanied by a significant red shift (>15 nm) and hypochromicity (40−55%) of the Soret absorption band. The exact extent of the red shift is difficult to determine because of the binding-induced distortion of the original Gaussian shape of the Soret band. Inspection of graphs a−c in Figure 3 reveals that the porphyrins' association with poly(rI)poly(rC) is accompanied by a rather modest red shift (>15 nm) and significant hypochromicity (25−45%) of the Soret band. We propose that the observed spectrophotometric changes may correspond to different binding modes since the quantitative distinctions between the three modes are somewhat blurred. (In addition, they may depend on the specific porphyrin and/or the host DNA or RNA.) CD

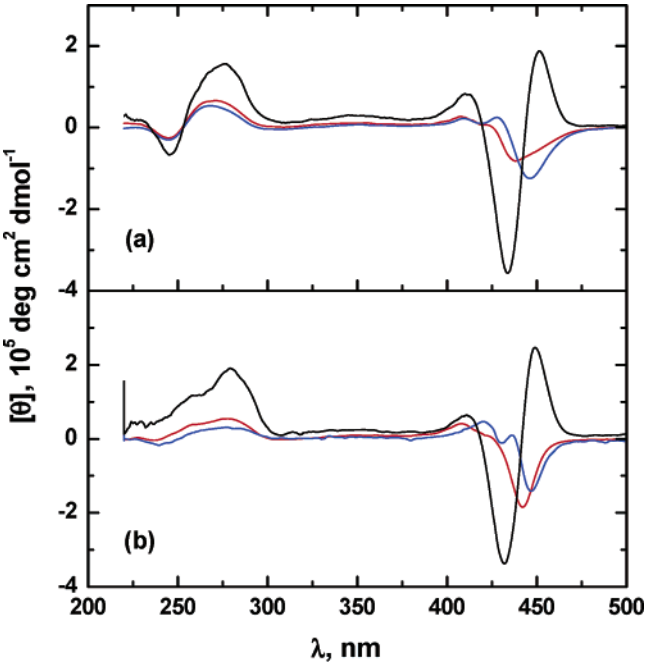

Figure 6. Circular dichroism spectra of poly(rA)poly(rU) (panel a) and poly(rI)poly(rC) (panel b) saturated with TEtOHPyP4 (red), TAlPyP4 (blue), and TMetAlPyP4 (black) at 25 °C.

offers a more robust and unequivocal way for discriminating between the three binding modes of porphyrin−nucleic acid interactions. In this regard, inspection of Figure 6 reveals that the complexes of TEtOHPyP4 and TAlPyP4 with the poly(rA)poly(rU) and poly(rI)poly(rC) host duplexes are characterized by negative induced CD bands in the Soret region. This observation is consistent with the picture in which TEtOHPyP4 and TAlPyP4 intercalate between bases of poly(rA)poly(rU) and poly(rI)poly(rC). In contrast, the complexes of TMetAlPyP4 with the two host RNA duplexes exhibit strong conservative CD bands in the Soret region in which a negative peak is followed by an equally strong positive peak. This observation is consistent with TMetAlPyP4 forming external stacks along the poly(rA)poly(rU) and poly(rI)poly(rC) duplexes.

A further evidence for the CD-suggested modes of binding is provided by the fluorescence spectra presented in Figures 4 and 5. It has been shown that intercalation of H_2TMPyP4 (a close analogue of the porphyrins studied here, albeit with less bulky methyl peripheral substituents) into poly(dGdC)poly(dGdC) DNA duplex is accompanied by rather slight changes in intensity and spectrum of the Q-band fluorescence of the porphyrin.[17] On the other hand, outside binding of H_2TMPyP4 to poly(dAdT)poly(dAdT) results in a splitting and significant increase in intensity of the emission spectrum of the dye.[17] Inspection of the fluorescence spectra presented in Figures 4 and 5 reveals that the binding of TMetAlPyP4 to poly(rA)poly(rU) (see Figure 4c) and poly(rI)poly(rC) (see Figure 5c) results in splitting and substantial enhancement of the intensity of its emission spectrum, while spectral changes associated with the binding of TEtOHPyP4 and TAlPyP4 to the two RNA duplexes (see Figures 4a,b and 5a,b) are rather modest. On the basis of this observation as well as our CD data, we propose that TEtOHPyP4 and TAlPyP4 intercalate into poly(rA)poly(rU) and

(17) Kelly, J. M.; Murphy, M. J.; Mcconnell, D. J.; Ohuigin, C. A *Nucleic Acids Res.* **1985**, *13*, 167−184.

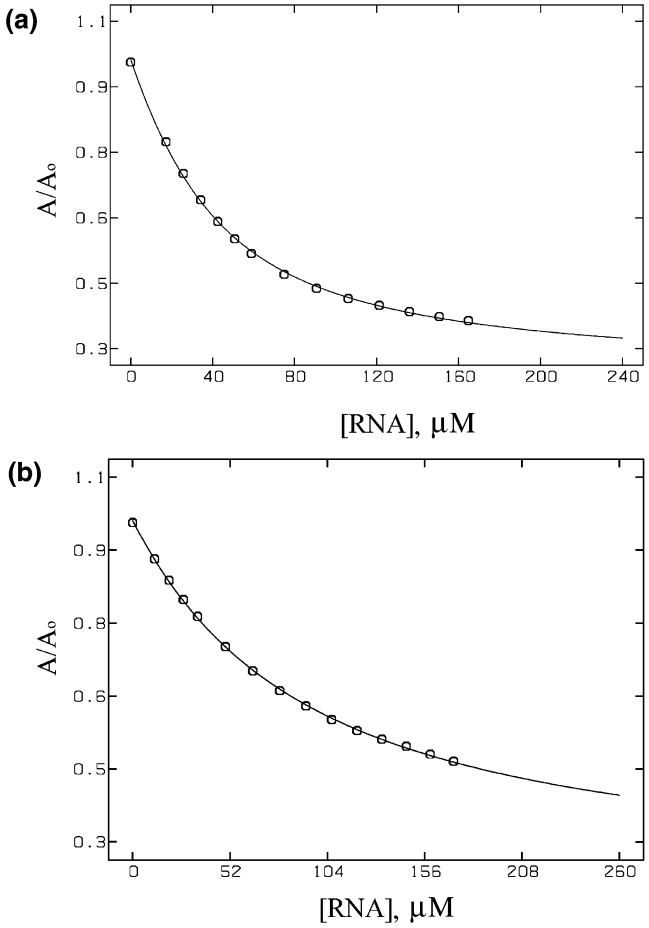

Figure 7. Representative binding profiles (absorption at 422 nm plotted versus total RNA concentration) for TEtOHPyP4 association with poly(rA)poly(rU) (panel a) and poly(rI)poly(rC) (panel b) at 25 °C. Experimental points were fit numerically with eq 1 (solid lines).

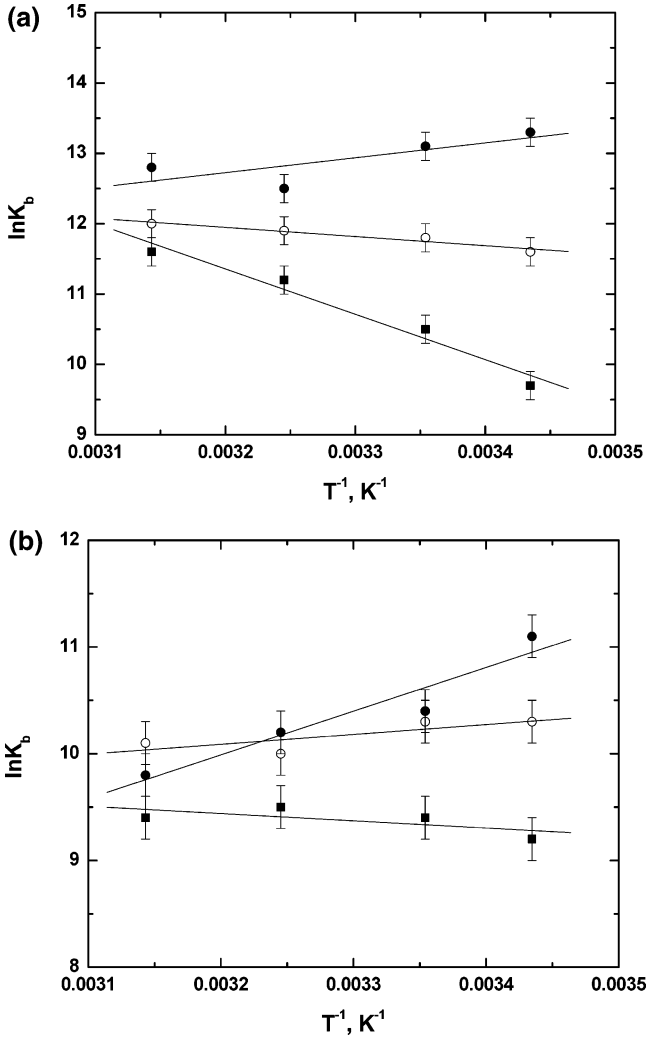

Figure 8. Temperature dependences of the binding constant for the associations of TEtOHPyP4 (●), TAlPyP4 (○), and TMetAlPyP4 (■) with poly(rA)poly(rU) (panel a) and poly(rI)poly(rC) (panel b).

Table 1. Thermodynamic Parameters of Porphyrin Binding to Poly(rA)Poly(rU) at 25 °C

porphyrin	n	K_b 10^5 M^{-1}	ΔG_b kcal mol^{-1}	ΔH_b kcal mol^{-1}	ΔS_b cal mol^{-1} K^{-1}
TEtOHPyP4	1.9 ± 0.2	4.9 ± 0.6	−7.8 ± 0.1	−4.2 ± 0.4	12.1 ± 1.4
TAlPyP4	1.8 ± 0.2	1.3 ± 0.2	−7.0 ± 0.1	2.6 ± 0.4	32.2 ± 1.4
TMetAlPyP4	3.4 ± 0.2	0.36 ± 0.02	−6.2 ± 0.1	12.8 ± 0.8	63.8 ± 2.8

Table 2. Thermodynamic Parameters of Porphyrin Binding to Poly(rI)Poly(rC) at 25 °C

porphyrin	n	K_b 10^5 M^{-1}	ΔG_b kcal mol^{-1}	ΔH_b kcal mol^{-1}	ΔS_b cal mol^{-1} K^{-1}
TEtOHPyP4	1.9 ± 0.3	0.34 ± 0.03	−6.2 ± 0.1	−8.1 ± 0.4	−6.4 ± 1.4
TAlPyP4	2.6 ± 0.2	0.30 ± 0.02	−6.1 ± 0.1	−1.8 ± 0.4	14.4 ± 1.4
TMetAlPyP4	3.0 ± 1.5	0.12 ± 0.02	−5.6 ± 0.1	1.4 ± 0.8	23.5 ± 2.8

poly(rI)poly(rC), while TMetAlPyP4 forms an outside type, self-stacked complexes with these duplexes.

The proposed modes of binding for TEtOHPyP4, TAlPyP4, and TMetAlPyP4 differ from the modes of association of H_2-TMPyP4 with the poly(rA)poly(rU) and poly(rI)poly(rC) duplexes.[8] It has been found that H_2TMPyP4 forms external self-stacks around poly(rI)poly(rC).[8] At low porphyrin-to-RNA ratios, *r*, H_2TMPyP4 forms external stacks around poly(rA)-poly(rU) while intercalating when *r* becomes higher than 0.3.[8] It is difficult to speculate about the molecular origins of that TEtOHPyP4 and TAlPyP4 with their bulky peripheral substituents ($-CH_2-CH_2-OH$ and $-CH_2-C(-CH_3)=CH_2$, respectively) intercalate into poly(rI)poly(rC), while H_2TMPyP4 with its methyl $-CH_3$ group does not. However, it should be noted that the bulkiness of the peripheral groups may not be the decisive factor in determining the binding pattern of a porphyrin. Recall that substitution of methyl groups in H_2TMPyP4 by 2-hydroxyethyl and propyl groups does not alter the binding preferences of the porphyrin with respect to the poly(dAdT)-poly(dAdT) and poly(dGdC)poly(dGdC) DNA duplexes.[10,11] Thus, the chemical structure of peripheral substituents appears to play a more important role than merely their size in determining the binding preferences of porphyrins.

Binding Affinities. Data in Tables 1 and 2 reveal that our determined porphyrin−RNA binding constants at 25 °C vary between 1.2×10^4 and 4.9×10^5 M^{-1}, a range typical for porphyrin−nucleic acid interactions.[4,8,9] Independent of the binding mode, each porphyrin studied here associates more tightly with poly(rA)poly(rU) than with poly(rI)poly(rC). For example, TEtOHPyP4 intercalates into poly(rA)poly(rU) and poly(rI)poly(rC) with binding constants of 4.9×10^5 and 3.4×10^4 M^{-1}, respectively, while TAlPyP4 intercalates with binding constants of 1.3×10^5 and 3.0×10^4 M^{-1}, respectively. TMetAlPyP4 binds to poly(rA)poly(rU) and poly(rI)poly(rC)

with binding constants of 3.6×10^4 and 1.2×10^4 M^{-1}, respectively. Molecular origins of the observed differential affinity of the two RNA duplexes for the porphyrins are yet to be uncovered.

It is instructive to compare the binding characteristics of TEtOHPyP4, TAlPyP4, and TMetAlPyP4 with those of their more compact analogue H_2TMPyP4. Recall that H_2TMPyP4 binds externally to poly(rI)poly(rC), while exhibiting two modes of binding (intercalation and outside binding) to poly(rA)poly(rU).[8] Intercalation of H_2TMPyP4 into poly(rA)poly(rU) is characterized by a binding constant of 6.8×10^5 M^{-1}, which is somewhat higher than 4.9×10^5 and 1.3×10^5 M^{-1}, the values exhibited by TEtOHPyP4 and TAlPyP4. This observation is consistent with an expectation that, based on steric considerations, H_2TMPyP4 with its compact peripheral methyl $-CH_3$ groups should intercalate more readily than TEtOHPyP4 with its bulky hydroxyethyl $-CH_2-CH_2-OH$ groups. However, it should be noted that porphyrins, being much larger than conventional intercalators, do not intercalate in a "normal" way. As shown by Williams and co-workers, intercalation of CuTMPyP4 into the $(dCGATCG)_2$ DNA duplex is accompanied by a severe conformational distortion of the DNA due to steric clashes between its backbone and the pyridinium groups of the porphyrin.[19] The porphyrin "hemiintercalates" between the CG steps within one strand of DNA but not the other. More importantly, the porphyrin does not form any appreciable van der Waals contacts with adjacent bases. Instead, the porphyrin−DNA complex is stabilized by extensive electrostatic interactions in the minor groove, where two positively charged pyridinium groups are located in close proximity to negatively charged phosphate oxygens. The other two pyridinium groups reside in the major groove of the complex and are relatively far away from the phosphate groups of the DNA. The fact that the pyridinium groups along with their peripheral atomic groups are located in the grooves of the duplex may suggest that the binding affinity does not necessarily correlate with the size of the peripheral groups. The chemical composition of the peripheral groups may represent a more important factor than their size since the former determines the host of DNA−porphyrin interactions in the grooves.

The outside binding of TMetAlPyP4 to poly(rI)poly(rC) is characterized by a binding constant of 1.2×10^4 M^{-1}, more than 2 orders of magnitude lower than 8.5×10^6 M^{-1}, the value determined for H_2TMPyP4−poly(rI)poly(rC) association.[8] This large disparity is consistent with the bulky $-CH_2-C(-CH_3)=CH_2$ peripheral groups of TMetAlPyP4 sterically impeding its approach to the RNA duplex with subsequent formation of self-stacks along the helix. This "explanation" is also consistent with the association of TMetAlPyP4 with poly(rA)poly(rU) that exhibits a binding constant of $K_b = 3.6 \times 10^4$ M^{-1}, comparable to that observed for the porphyrin binding to poly(rI)poly(rC) (see Table 1).

Binding Enthalpies. The majority of intercalating agents, including porphyrins, studied to date exhibit negative changes in enthalpy upon their association with nucleic acids.[20−22] For example, intercalation of H_2TMPyP4 into three oligomeric G-tetraplexes differing in length and composition is accompanied by favorable changes in enthalpy.[6] Intercalation of this porphyrin and its metaloderivative CuTMPyP4 into calf thymus DNA also causes favorable changes in enthalpy of −4.6 and −5.9 kcal mol^{-1}, respectively.[23] On the other hand, the binding of ZnTMPyP4, an outside binder, to the same DNA causes an unfavorable change in enthalpy of 1.5 kcal mol^{-1}.[23]

A favorable change in enthalpy upon porphyrin intercalation is consistent with a picture in which the bound porphyrin forms strong intermolecular interactions with the host DNA. However, X-ray crystallographic studies have revealed that porphyrin does not form any appreciable interactions with adjacent bases.[19] Moreover, porphyrin intercalation results in a severe distortion of the host duplex that should cause disruption of some interstrand interactions.[19] These processes should contribute unfavorably to the binding enthalpy. Apparently, the favorable enthalpic contribution of strong electrostatic interactions between the positively charged pyridinium groups of the porphyrin and DNA phosphates prevails over the unfavorable contribution of disrupted and unformed interactions and results in a negative ΔH_b. On the other hand, external binding of porphyrins should not significantly alter the DNA or RNA structure. Unfavorable changes in enthalpy, ΔH_b, accompanying external porphyrin binding may, in part, reflect dehydration of some polar and charged groups of DNA without adequately supplying them by hydrogen bonds from the external porphyrin stacks.

This discussion and emerging thermodynamic picture are essentially consistent with our enthalpic data presented in Tables 1 and 2. Note that, for each RNA duplex, the binding enthalpy, ΔH_b, is the most favorable for TEtOHPyP4 (an intercalator) followed by TAlPyP4 (an intercalator) and TMetAlPyP4 (an outside binder). Intercalation of TEtOHPyP4 to the poly(rA)poly(rU) and poly(rI)poly(rC) host duplexes is accompanied by highly favorable enthalpy changes of −4.2 and −8.1 kcal mol^{-1}, respectively. External binding of TMetAlPyP4 to poly(rA)poly(rU) and poly(rI)poly(rC) is accompanied by unfavorable enthalpy changes of 12.8 and 1.4 kcal mol^{-1}. On the other hand, intercalation of TAlPyP4 into poly(rA)poly(rU) is accompanied by a slightly positive change in enthalpy of 2.6 kcal mol^{-1}, while its intercalation into poly(rI)poly(rC) causes a slightly negative change in enthalpy of −1.8 kcal mol^{-1}. As a working hypothesis, we propose that favorable (electrostatic interactions) and unfavorable (duplex distortion) contributions to the binding enthalpy for TAlPyP4 intercalation nearly compensate each other, producing either slightly negative or slightly positive values of ΔH_b.

Binding Entropies. Further inspection of Tables 1 and 2 reveals that all porphyrin−RNA association events studied here, with an exception of TEtOHPyP4 binding to poly(rI)poly(rC), are accompanied by favorable changes in entropy, ΔS_b, ranging from 12.1 to 63.2 cal mol^{-1} K^{-1}. Intercalation of TEtOHPyP4 into poly(rI)poly(rC) is accompanied by a slightly negative change in entropy of −6.1 cal mol^{-1} K^{-1}. Significantly, for each RNA duplex, external self-stacking of TMetAlPyP4 produces the most favorable values of ΔS_b. Thus, analogous to

(18) Pasternack, R. F. *Chirality* **2003**, *15*, 329−332.
(19) Lipscomb, L. A.; Zhou, F. X.; Presnell, S. R.; Woo, R. J.; Peek, M. E.; Plaskon, R. R.; Williams, L. D. *Biochemistry* **1996**, *35*, 2818−2823.
(20) Chaires, J. B. *Biopolymers* **1997**, *44*, 201−215.
(21) Ren, J. S.; Jenkins, T. C.; Chaires, J. B. *Biochemistry* **2000**, *39*, 8439−8447.
(22) Chou, W. Y.; Marky, L. A.; Zaunczkowski, D.; Breslauer, K. J. *J. Biomol. Struct. Dyn.* **1987**, *5*, 345−359.
(23) Pasternack, R. F.; Garrity, P.; Ehrlich, B.; Davis, C. B.; Gibbs, E. J.; Orloff, G.; Giartosio, A.; Turano, C. *Nucleic Acids Res.* **1986**, *14*, 5919−5931.

binding enthalpy, ΔH_b, binding entropy, ΔS_b, appears to correlate with the binding mode.

A change in entropy, ΔS_b, accompanying a protein or nucleic acid binding event can be presented as the sum of intrinsic (configurational), ΔS_{conf}, hydration, ΔS_{hyd}, and rotational and translational, ΔS_{rt}, contributions:[24]

$$\Delta S_b = \Delta S_{conf} + \Delta S_{hyd} + \Delta S_{rt} \quad (2)$$

The term ΔS_{rt} is generally unfavorable. For the association of DNA with a cationic drug, the term ΔS_{rt} contains, however, a favorable polyelectrolyte contribution due to dissociation of condensed counterions.[25−27] The configurational term, ΔS_{rt}, may be either negative (unfavorable) or positive (favorable) depending on whether the ligand and the host duplex "rigidify" or "loosen" upon their association. The sign of the hydration contribution, ΔS_{hyd}, depends on whether water molecules are predominantly released from or taken up by the hydration shells of the reacting species.

Our recent study has revealed that intercalation of ethidium bromide, a prototypical intercalator, into the poly(dAdT)poly(dAdT), poly(dGdC)poly(dGdC), and poly(dIdC)poly(dIdC) duplexes is accompanied by unfavorable changes in configurational entropy, ΔS_{conf}, ranging from −15.4 to −33.6 cal mol^{-1} K^{-1}.[28] This result suggests that ethidium binding brings about a rigidifying of the resulting drug−DNA complex. Perhaps, it would be plausible to assume that the intercalation of TEtOHPyP4 and TAlPyP4 into the poly(rA)poly(rU) and poly(rI)poly(rC) duplexes also results in a decrease in configurational entropy. However, the effect should be smaller than that observed for ethidium intercalation due to severe structural distortion of porphyrin−duplex complexes as observed by Williams and co-workers.[19]

In a number of recent publications, we have applied volumetric measurements to characterize changes in hydration accompanying protein−ligand and DNA−ligand association events.[28−31] For all association reactions that have been studied, we have observed a net release of water from the hydration shells of the interacting species and, consequently, a favorable change in hydration entropy, ΔS_{hyd}. For example, for ethidium intercalation into the poly(rA)poly(rU), poly(dAdT)poly(dAdT), poly(dGdC)poly(dGdC), and poly(dIdC)poly(dIdC) duplexes as well as to the poly(rU)poly(rA)poly(rU) triplex, ΔS_{hyd} has been found to be within the range of 4.6−30.6 cal mol^{-1} K^{-1}.[28] By extension, as a working hypothesis, we propose that the major favorable contribution to the binding entropy comes from dehydration of porphyrin and RNA groups upon their association. Clearly, external stacking of TMetAlPyP4 along the duplex helices should be accompanied by more extensive burial of previously solvent-exposed atomic group and, consequently, more extensive dehydration than intercalation of TEtOHPyP4 and TAlPyP4. This rationalization is consistent with more favorable ΔS_b values observed for TMetAlPyP4 compared to those observed for TEtOHPyP4 and TAlPyP4.

Concluding Remarks

We studied the interactions of *meso*-tetrakis(4*N*-(2-hydroxyethyl)pyridinium-4-yl) porphyrin (TEtOHPyP4), *meso*-tetrakis(4*N*-allylpyridinium-4-yl) porphyrin (TAlPyP4), and *meso*-tetrakis(4*N*-metallylpyridinium-4-yl) porphyrin (TMetAlPyP4) with the poly(rA)poly(rU) and poly(rI)poly(rC) homopolymeric RNA duplexes at 18, 25, 35, and 45 °C. To this end, we employed circular dichroism, light absorption, and fluorescence intensity spectroscopic measurements. Our combined CD and fluorescence results suggest that TEtOHPyP4 and TAlPyP4 intercalate into poly(rA)poly(rU) and poly(rI)poly(rC), while TMetAlPyP4 forms outside-bound, self-stacked aggregates along the RNA helices.

We used our Soret absorption titration data to construct the binding profile for each porphyrin−RNA association event studied in the present paper. These profiles were analyzed directly using numerical calculations using the neighbor-exclusion model to determine the binding constants and stoichiometry for each porphyrin−RNA binding. From temperature-dependent data on of the binding constants, we evaluated the binding free energies, ΔG_b, enthalpies, ΔH_b, and entropies, ΔS_b. Independent of the binding mode, each porphyrin studied here associates more tightly with poly(rA)poly(rU) than with poly(rI)poly(rC). For each host RNA duplex, the binding enthalpy, ΔH_b, is the most favorable for TEtOHPyP4 (an intercalator) followed by TAlPyP4 (an intercalator) and TMetAlPyP4 (an outside binder). On the other hand, for each duplex, external self-stacking of TMetAlPyP4 produces the most favorable change in entropy, ΔS_b, followed by the intercalators TAlPyP4 and TEtOHPyP4.

We compared the binding properties of TEtOHPyP4, TAlPyP4, and TMetAlPyP4 containing bulky peripheral groups with those reported for their analogue H_2TMPyP4 with more compact methyl peripheral substituents. This comparison revealed that both the binding mode and binding affinities of the porphyrins may be modulated by the peripheral groups. In such modulations, the chemical nature of the peripheral substituent appears to be more important than its size.

Taken together, our results suggest that the thermodynamic profile of the porphyrin−RNA binding correlates with the binding mode. This correlation reflects the differential nature of the molecular forces that stabilize/destabilize the two modes of binding—intercalation versus external self-stacking along the host duplex. In general, thermodynamic results presented in this work, in conjunction with previous thermodynamic data on porphyrin−nucleic acid interactions, may prove useful in developing strategies for rational design of porphyrin-based ligands targeted with predictable affinity and specificity to selected nucleic acid sites.

Acknowledgment. We thank Dr. Robert B. Macgregor, Jr. for his useful comments and stimulating discussions. This work was supported by grants from the Canadian Institutes of Health Research to T.V.C. and J.W.W., and from NATO (Collaborative Linkage Grant LST.CLG.979777) to T.V.C. and S.G.H.

JA054070N

(24) Luque, I.; Freire, E. *Methods Enzymol.* **1998**, *295*, 100−127.
(25) Manning, G. S. *Q. Rev. Biophys.* **1978**, *1*, 179−246.
(26) Record, M. T.; Anderson, C. F.; Lohman, T. M. *Q. Rev. Biophys.* **1978**, *11*, 103−178.
(27) Tikhomirova, A.; Chalikian, T. V. *J. Mol. Biol.* **2004**, *341*, 551−563.
(28) Han, F.; Chalikian, T. V. *J. Am. Chem. Soc.* **2003**, *125*, 7219−7229.
(29) Filfil, R.; Chalikian, T. V. *FEBS Lett.* **2003**, *554*, 351−356.
(30) Dubins, D. N.; Filfil, R.; Macgregor, R. B.; Chalikian, T. V. *J. Phys. Chem. B* **2000**, *104*, 390−401.
(31) Chalikian, T. V.; Plum, G. E.; Sarvazyan, A. P.; Breslauer, K. J. *Biochemistry* **1994**, *33*, 8629−8640.